Mixed-basis band-structure interpolation scheme applied to the fluorite-structure compounds $NiSi_2$, $AuAl_2$, $AuGa_2$, and $AuIn_2$

Sehun Kim, Jeffrey G. Nelson, and R. Stanley Williams
Department of Chemistry and Biochemistry, University of California, Los Angeles, Los Angeles, California 90024
(Received 6 August 1984)

A mixed-basis band-structure interpolation scheme for fcc *d*-band metals has been extended to include fluorite-structure (CaF_2) compounds by incorporating more plane waves in the basis set. Since the fluorite and fcc structures belong to the same space group, the interpolation scheme originally developed for fcc *d*-band metals is also capable of generating fluorite band structures. The interpolation parameters for $NiSi_2$, $AuAl_2$, $AuGa_2$, and $AuIn_2$ have been determined by fitting nonrelativistic first-principles calculations using a nonlinear least-squares procedure. Good agreement with the first-principles results is obtained up to about 5 eV above the Fermi level for a basis set containing 39 plane waves and 5 *d* functions. The parameters for the intermetallic compounds containing Au were then adjusted to include the effects of spin-orbit splitting in the *d* bands and to improve the agreement of the calculated density of states with the results of photoelectron spectra. The adjusted *d* bands of $AuAl_2$, $AuGa_2$, and $AuIn_2$ differ considerably from those calculated by first principles.

I. INTRODUCTION

Mixed-basis band-structure interpolation schemes have proven to be extremely valuable computational tools for the study of the electronic structure of *d*-band metals. The first routines were developed by Hodges, Ehrenreich, and Lang[1] and Mueller[2] for simple fcc *d*-band metals. Smith and co-workers[3–6] have continued the development of an fcc *d*-band interpolation scheme over the past decade and have applied it as an aid in interpreting photoemission and uv reflectance data. The advantages in using such a second-principles technique are the following: (1) it is simple and inexpensive to generate E versus $\mathbf{k}$ and densities-of-states plots; (2) the parameters in an interpolation scheme may be easily adjusted to improve the agreement between the calculated energy bands and experimental observations; and (3) the parameters may be reported in the literature and used by other investigators to generate the identical band structure, which makes the results of a band-structure determination very portable. Furthermore, Smith and co-workers have shown that transition-matrix elements calculated using the parametrized Hamiltonian agree reasonably well with observed spectral intensities in reflectance and angle-resolved photoemission spectroscopy (ARPES).[5,6] By fitting a band-structure interpolation scheme to experimental data, it should be possible to experimentally determine the electronic structure of solids to a high degree of accuracy.

In this paper the interpolation scheme of Smith *et al.*[3–6] is extended further to more complex systems, i.e., the fluorite structure compounds AB_2, which have larger and more complex unit cells than the fcc *d*-band metals. The fluorite structure is composed of one A and two B fcc sublattices, with one B sublattice translated by one-fourth the body diagonal of the cubic unit cell along both the [111] and $[\bar{1}\,\bar{1}\,\bar{1}]$ directions with respect to the A sublattice. Several intermetallic compounds involving Au and Pt (the A elements of AB_2) and the technologically important silicides $NiSi_2$ and $CoSi_2$ have the fluorite structure. In these cases, the A atoms have valence *d* orbitals that are very important in determining the electronic structure of the compounds, but the *d* contribution of the B atoms is probably extremely small. Since the A atoms reside on an fcc sublattice with larger dimensions than in the corresponding elements, the *d*-*d* interactions in the compounds should be much smaller than in the elements. Thus it should be quite interesting to compare the *d*-band regions of the various intermetallic compounds with each other and with the corresponding fcc *d*-band metals. However, to date very few band-structure calculations have been performed on the *d*-band fluorite compounds.

At first, the application of an interpolation scheme to the fluorite compounds may seem complicated, but since the fluorite structure has the same space-group symmetry as fcc crystals, the mixed interpolation scheme developed for fcc *d*-band metals is also quite satisfactory for the fluorite structure. An interpolation scheme has been developed similar to that of Smith and co-workers[3–6] except that more plane waves were included in the basis set to enhance the convergence in the fitting procedure. Single-ζ Slater orbitals were used to approximate the radial part of the *d*-wave functions in calculating *d*-wave overlap integrals, but this approximation was no better than Smith's use of spherical Bessel functions for the overlap integral. Using a nonlinear least-squares procedure,[7] the interpolated bands may be fitted to the energy eigenvalues at high-symmetry points in the Brillouin zone (BZ) of first-principles calculations to determine the 19 parameters used in the interpolation scheme. The resulting band structures may be optimized by adjusting some of the fitting parameters to agree with experimental observations, and then compared with one another to analyze the effects of atomic structure and composition on electronic structure.

The main purpose of the research reported here was to determine how well a simple interpolation scheme could compute the band structure of the d-band fluorite compounds. In Sec. II the details of the present interpolation scheme are summarized. These include a description of the mixed interpolation scheme of Smith and coworkers,[3-6] the modification of the basis set, the single-ζ-type overlap integrals, and a summary of the nonlinear least-squares procedure.[7] In Sec. III the results of the application of the present scheme to fit nonrelativistic first-principles band-structure calculations for $NiSi_2$, $AuAl_2$, $AuGa_2$, and $AuIn_2$ are presented. Finally, Sec. IV contains a discussion of these results, an extension of the calculations to include spin-orbit effects and improve agreement with experimental results in the Au $5d$ bands of $AuAl_2$, $AuGa_2$, and $AuIn_2$, and a further comparison of the results to experimental data and band structures of the fcc metals, Ni and Au.

II. INTERPOLATION SCHEME AND FITTING PROCEDURE

This work basically adopts the mixed interpolation scheme developed by Smith and co-workers.[3-6] According to this scheme, the nonrelativistic Hamiltonian for fcc d-band metals is

$$H=\begin{bmatrix} H_{cc} & H_{cd} \\ H_{dc} & H_{dd} \end{bmatrix}, \tag{1}$$

where H_{cc}, H_{cd}, and H_{dd} represent the plane wave, the hybridization, and the d-orbital tight-binding blocks, respectively.

All of these blocks retain the same parametrized forms as in the interpolation scheme of Smith and co-workers.[3-6] However, the plane-wave block of H_{cc} has been extended to a 39×39 rather than 16×16 submatrix in order to reproduce the valence-band structure of the fluorite compounds. In terms of the reduced wave vector $\mathbf{k}$, the 39 plane waves included in the basis set are those with wave vectors $\mathbf{k}_i=\mathbf{k}+\mathbf{G}_i$, where $\mathbf{k}$ is constrained to be within the first BZ and $\mathbf{G}_i$ includes the reciprocal-lattice vector (0,0,0), all eight vectors of the type $(2\pi/a)(\pm1,\pm1,\pm1)$, all six of the type $(2\pi/a)(\pm2,0,0)$, all 12 of the type $(2\pi/a)(\pm2,\pm2,0)$, and all 12 of the type $(2\pi/a)(-3,\pm1,\pm1)$.

The Hamiltonian elements of the plane-wave block, H_{cc}, are expressed in the same form as in Smith's scheme,

$$H_{ij}=\alpha k_i^2\delta_{ij}+V_{ij}+Sj_2(k_iR)j_2(k_jR)P_2(\mathbf{k}_i\cdot\mathbf{k}_j)\ . \tag{2}$$

The first term is the free-electron energy in which $\alpha=(\hbar^2/2m)(\pi/4a)^2$ and a is the lattice constant. The V_{ij} are local pseudopotential terms, of which the lowest six, V_{000}, V_{111}, V_{200}, V_{220}, V_{311}, and V_{222}, are assumed to be nonzero. The parameter S is a constant in the orthogonalization term, j_2 is the usual spherical Bessel function of order 2, and P_2 is the Legendre polynomial of the order of 2. The S term may be regarded as a nonlocal pseudopotential and the parameter R as a muffin-tin radius; both are treated as disposable parameters for this scheme.

The form of the local pseudopotential in the plane-wave portion of the parametrized Hamiltonian for the fluorite structure may be expected to differ from that for fcc metals. The total local pseudopotential of AB_2 can be written as follows:

$$V_{\mathbf{G}}(AB_2)=V_{\mathbf{G}}(A)+V_{\mathbf{G}}(B)\cos(\mathbf{G}\cdot\boldsymbol{\tau})\ , \tag{3}$$

where $\boldsymbol{\tau}=(a/4)(1,1,1)$ and $\boldsymbol{\tau}$ is a vector connecting an A atom to one of the B atoms in the primitive unit cell (the other B atom is at $-\boldsymbol{\tau}$) of the fluorite lattice structure. The $V_{\mathbf{G}}(A)$ and $V_{\mathbf{G}}(B)$ pseudopotential terms are in principle dependent only on the identity of the A and B atoms, respectively. For the $\mathbf{G}$ vectors of the reciprocal lattice of the fluorite structure, the values of $\cos(\mathbf{G}_i\cdot\boldsymbol{\tau})$ are limited to -1, 0, or 1 and are determined only by the magnitude of $\mathbf{G}_i$, not its direction. Although Eq. (3) is expressed as a sum of the pseudopotential coefficients for two different atoms, the total local pseudopotential has exactly the same functional form as the pseudopotential parameters in Smith's fcc d-band scheme. Thus the values of $V_{\mathbf{G}_i}$ for AB_2 are all constants, with

$$V_{\mathbf{G}_i}(AB_2)=\begin{cases} V_{\mathbf{G}_i}(A)-V_{\mathbf{G}_i}(B) & \text{for } |G_i|=2,\sqrt{12}\ , \\ V_{\mathbf{G}_i}(A) & \text{for } |G_i|=\sqrt{3},\ \sqrt{11}\ , \\ V_{\mathbf{G}_i}(A)+V_{\mathbf{G}_i}(B) & \text{for } |G_i|=8,\ 4\ , \end{cases} \tag{4}$$

where $|G_i|$ is in units of $2\pi/a$. As long as the d-orbital contribution of the B atoms to the band structure is negligible, the interpolation Hamiltonian of the fluorite structure is identical to that of the fcc structure.

The Hamiltonian elements of the hybridization block, H_{cd}, are expressed in the following form:

$$H_{ij}=B_{t,e}j_2(kR)Y_j(\mathbf{k}_i)\ , \tag{5}$$

where B_t and B_e are constants in the hybridization terms that are treated as disposable parameters for orbitals with t_{2g} and e_g symmetry, respectively. The functions $Y_j(\mathbf{k}_i)$ represent the set of real spherical harmonics. The spherical Bessel functions in Eqs. (2) and (5) are overlap integrals involving the radial parts of the d orbitals and plane waves in which the function $r^2R_{nd}(r)$ is approximated by a δ function. A possible improvement to the overlap integral might be to approximate $R_{nd}(r)$ with Slater wave functions. The resulting overlap integrals used in this work are listed in Appendix A. In the fitting procedure, the initial value of the orbital exponent, ζ, was taken from the tables of Clementi and Roetti[8] for the appropriate atomic d-wave function, after which ζ was treated as a disposable parameter in the fitting procedure.

The matrix elements of the H_{dd} block may be expressed in the tight-binding forms given by Slater and Koster[9] or Fletcher and Wohlfarth.[10] The nearest-neighbor three-center form of Fletcher[11] was used in the present scheme. The Fletcher notation[11] involves eight parameters: E_0, Δ, A_1, A_2, A_3, A_4 A_5, and A_6. The A parameters specify the dispersion of the bands, while E_0 and $E_0+\Delta$ are the mean energies of the t_{2g} and e_g subbands, respectively.

For relativistic band-structure calculations, the effect of spin-orbit coupling on the d bands may be included in the

manner of Friedel *et al.*[12] The total Hamiltonian has the following form:

$$H_{\text{rel}}=\begin{bmatrix} H_{cc} & H_{cd} & 0 & 0 \\ H_{dc} & H_{dd}+\xi M & 0 & \xi N \\ 0 & 0 & H_{cc} & H_{cd} \\ 0 & -\xi N^{*} & H_{dc} & H_{dd}-\xi M^{*} \end{bmatrix}, \tag{6}$$

where M and N are given by Friedel *et al.*[12] The spin-orbit splitting parameter ξ may be determined from ARPES measurements[13] or be taken from atomic values.

The parameters of the mixed interpolation scheme for a particular system were determined by appling a nonlinear least-squares procedure[7] to fit the energy eigenvalues of first-principles calculations.[14–16] In this fitting procedure, each energy eigenvalue was given equal weight regardless of its degeneracy. The parameters of Ni and Au given by Smith *et al.*[3,17] were used as an initial guess of the parameters for the fluorite structure compounds, except that the α and R parameters were changed to reflect the different lattice constants of the intermetallic compounds, where α is proportional to $1/a^2$ and R is expressed as a fraction of a. Using this procedure, the parameters usually converged to values which yielded a root-mean-square (rms) error in the energy bands of the fluorite structure compounds of about 0.15 eV after 3–4 iterations.

After the fitting parameters for a band structure were determined, the total density of states (TDOS) of the system was obtained by summing a set of Gaussian peaks with a 0.3 eV full width at half maximum that were centered at the energy eigenvalues calculated at 60 special points[18] in the BZ. These special points were chosen to efficiently calculate averages over the BZ of periodic functions of the wave vector.[18] The TDOS plots may then be compared to x-ray photoemission (XPS) data or other probes which sample an average over the valence or conduction bands.

All the calculations were performed using a VAX 11/780 computer. The central processing unit (CPU) time of the VAX required to produce the eigenvalues at a single k point for nonrelativistic and relativistic calculations was 3.7 and 33 s, respectively, for the cases in which the H_{cc} blocks contained 39 plane waves.

III. RESULTS

The number of first-principles band structures for d-band fluorite compounds is limited to nonrelativistic augmented-plane-wave (APW) calculations for Au intermetallic compounds with Al, Ga, and In (Ref. 14) and $NiSi_2$.[15,16] The energy bands generated by the interpolation scheme and the TDOS for $NiSi_2$, $AuAl_2$, $AuGa_2$, and $AuIn_2$ are illustrated in Figs. 1–4, respectively. The fitting procedure utilized 33–39 energy eigenvalues taken from the APW results[14–16] at 4–5 symmetry points.

The main difference between $NiSi_2$ and the Au alloys is that in $NiSi_2$, the d bands mix strongly with the plane-wave states, whereas the d bands in the Au alloys essentially reside in a band gap of the plane-wave states. One

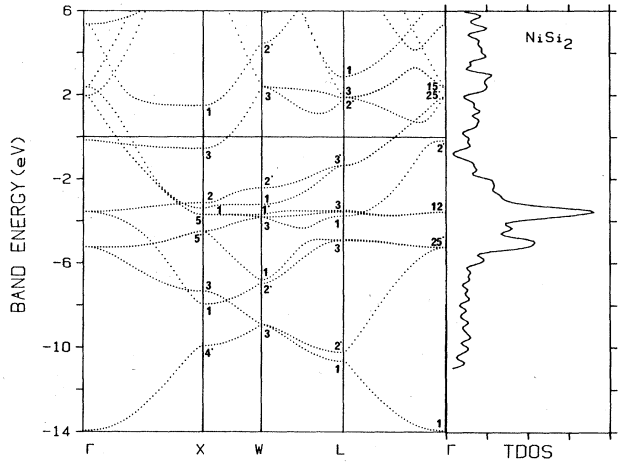

FIG. 1. Energy bands of $NiSi_2$ generated using the parameters of Table I and plotted along high-symmetry lines in the fcc Brillouin zone. Also shown is the corresponding TDOS. The energy scale is referenced to the Fermi energy and the TDOS scale has arbitrary units.

especially noteworthy feature associated with $AuGa_2$ is the flat band with Δ_2 symmetry calculated by the APW procedure of Switendick and Narath[14] and reproduced by the interpolation scheme in Fig. 3. In Figs. 5 and 6, the effects of including spin-orbit coupling in the d bands of $AuGa_2$ and $AuIn_2$ as well as adjusting the d bands to agree with ARPES data[13] by varying the E_0 and Δ parameters are shown.

In Fig. 7, the TDOS for $AuAl_2$, $AuGa_2$, and $AuIn_2$ are compared with the corresponding XPS data.[19] In this comparison, the raw experimental data with no background subtraction are displayed. For each compound, two TDOS curves calculated using the interpolation scheme are shown: one for the fit to first-principle's results and the other for the empirically adjusted d bands (for $AuAl_2$, the $AuGa_2$ spin-orbit coupling parameter was

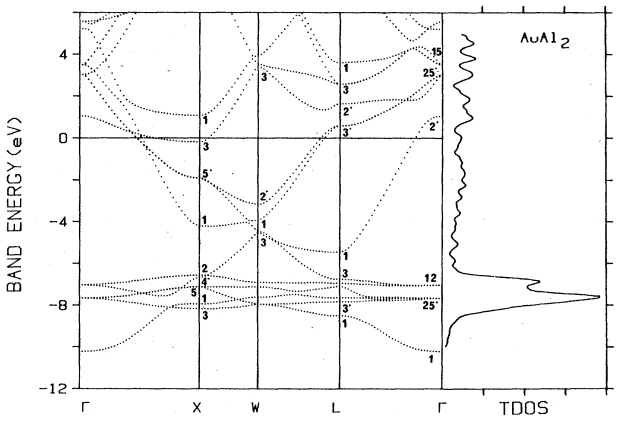

FIG. 2. Energy bands and TDOS of $AuAl_2$ with the same remarks as Fig. 1.

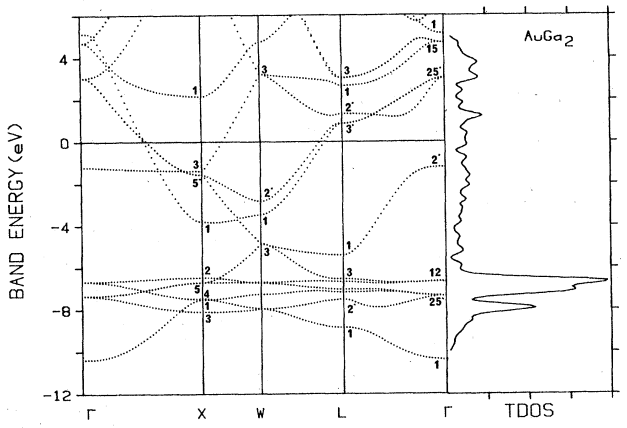

FIG. 3. Energy bands and TDOS of $AuGa_2$ with the same remarks as Fig. 1.

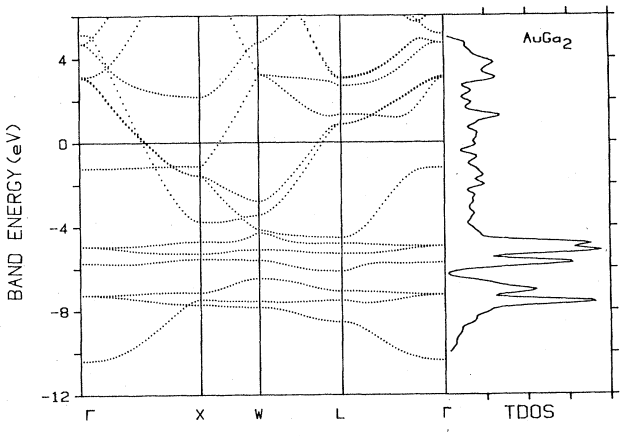

FIG. 5. Energy bands and TDOS of $AuGa_2$ with spin-orbit interactions in the d bands and adjustments to agree with the ARPES data of Ref. 13.

used and the E_0 and Δ parameters were adjusted to enhance the agreement with the XPS data of Ref. 19). A Gaussian broadening of 1.0 eV was applied to all these TDOS curves to roughly simulate the total experimental resolution of the spectra.

The parameters determined from the fitting procedure for the fluorite compounds are listed in Table I, along with the standard deviation for each parameter determined by the fitting procedure. For the purpose of comparison, this table also lists the parameters of Ni and Au calculated by this scheme for 39 plane waves in the H_{cc} block. Some of the A parameters for the fluorite compounds have negative values, unlike those of the fcc d metals, but in most of these cases the uncertainty in determining the negative values is as large as those A parameters (i.e., they are effectively zero). Both the B hybridization and S orthogonalization parameters of the intermetallic compounds are smaller than those of the fcc metals. The pseudopotential coefficients V_{200}, V_{220}, and V_{311} of the compounds are larger and V_{222} is smaller than those of the corresponding fcc metals, which is the result of the contribution to the pseudopotential of the Si or group-III atoms in the compounds. As expected from Sec. II, the values of V_{111} for $NiSi_2$ and Ni are nearly identical, since the form factor of the pseudopotential of the B atoms in AB_2 is zero. However, for all other cases involving $NiSi_2$ and the Au intermetallics, the values of V_{111} and V_{311} differ substantially.

The entries at the bottom of Table I indicate the rms errors and the average deviations for each of the fits. The rms errors in the fits to the Ni and Au energy bands are larger than those for $NiSi_2$ and Au alloys because more APW energy eigenvalues[20,21] (51 for Ni and 90 for Au) were used in the fitting procedure. The rms errors in the fits to the energy bands of the fcc metals using the present 39 orthogonalized plane-wave (OPW) scheme were less than those using Smith's original 16 OPW scheme. Thus increasing the number of plane waves in the basis set enables a substantial improvement in the fit to a band struc-

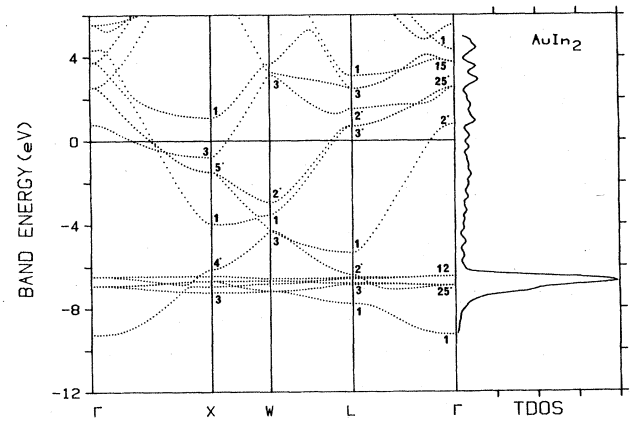

FIG. 4. Energy bands and TDOS of $AuIn_2$ with the same remarks as Fig. 1.

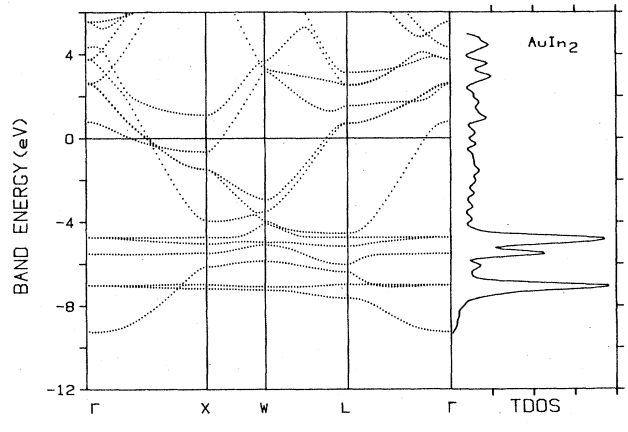

FIG. 6. Energy bands and TDOS of $AuIn_2$ with the same remarks as Fig. 5.

TABLE I. Parameters used in the mixed interpolation schemes.

Parameter[a]	Ni[b]	$NiSi_2$	Au[c]	$AuAl_2$[d]	$AuGa_2$[d]	$AuIn_2$[d]
E_0	8.218 ±0.3	4.681 ±0.4	3.775 ±0.02	0.4887±0.3	−0.0537±0.4	0.2609±0.4
				(1.1079)	(0.9112)	(0.9839)
Δ	−0.4190±0.4	0.5721±0.6	0.3078±0.3	0.0643±0.5	−0.2141±0.6	−0.8248±0.7
				(−0.1328)	(0.1077)	(0.5017)
A_1	0.2522±0.1	0.0020±0.01	0.2795±0.08	0.0054±0.2	0.0108±0.2	−0.0211±0.2
A_2	0.0849±0.08	0.0108±0.005	0.0433±0.06	0.0001±0.1	−0.0021±0.1	−0.0053±0.1
A_3	0.2196±0.1	0.0032±0.02	0.1498±0.1	−0.0144±0.2	0.5500±0.2	0.0123±0.2
A_4	0.2678±0.1	0.0254±0.05	0.0137±0.09	0.0725±0.1	0.0807±0.1	0.4356±0.1
A_5	0.0521±0.08	−0.0045±0.005	0.0509±0.06	0.0247±0.1	0.0110±0.2	0.0008±0.2
A_6	0.0664±0.2	−0.0179±0.003	0.2278±0.09	0.0567±0.1	0.0356±0.2	0.0200±0.2
α	0.1840±0.002	0.0776±0.002	0.1495±0.002	0.0655±0.002	0.0660±0.002	0.0611±0.002
V_{000}	0.7907±0.3	−3.727 ±0.3	−1.220 ±0.2	0.7010±0.3	−0.5653±0.3	0.5248±0.3
V_{111}	1.122 ±0.3	1.102 ±0.6	0.4541±0.2	3.018 ±0.4	2.537 ±0.3	2.665±0.3
V_{200}	1.157 ±0.2	2.806 ±0.3	−0.0583±0.2	3.643 ±0.3	3.748 ±0.2	3.372±0.2
V_{220}	0.1846±0.2	2.110 ±0.3	−0.5871±0.2	2.715 ±0.3	2.004 ±0.2	2.338±0.2
V_{311}	−0.1894±0.4	1.232 ±0.7	0.9521±0.4	2.282 ±0.6	2.038 ±0.3	2.241±0.3
V_{222}	0.1455±0.6	1.085 ±0.6	2.852 ±0.4	1.873 ±0.6	1.479 ±0.6	1.570±0.6
R	0.3169±0.02	0.2683±0.003	0.3192±0.01	0.2813±0.04	0.2776±0.05	0.2760±0.05
B_t	18.89 ±3	11.38 ±3	23.29 ±2	9.02 ±3	9.25 ±3	7.21±3
B_e	16.59 ±4	10.38 ±3	27.90 ±2	5.35 ±3	2.65 ±6	1.48±3
S	31.49 ±4	4.64 ±3	26.11 ±4	7.18 ±7	6.64 ±3	5.39±8
ξ			0.653	(0.777)	(0.777)	(0.748)
E_F[e]	9.25	8.15	7.21	7.56	6.60	6.80
Lattice constant (Å)	3.52	5.40	4.08	6.00	6.06	6.50
rms error	0.198	0.146	0.345	0.111	0.115	0.107
Average deviation	0.144	0.104	0.249	0.088	0.094	0.083

[a]All values in eV except R in a reduced unit and lattice constant in Å. The ± sign indicates the standard deviation of each parameter.
[b]Parameters are fitted to APW results from Ref. 19.
[c]Parameters are fitted to APW results from Ref. 20 with ξ from Ref. 5.
[d]Parameters in parentheses are adjusted to fit XPS data for $AuAl_2$ and ARPES data for $AuGa_2$ and $AuIn_2$ with the inclusion of spin-orbit coupling parameter ξ.
[e]From Refs. 14, 15, 17, and 20. In this scheme each E_F was used as an offset for the energy levels.

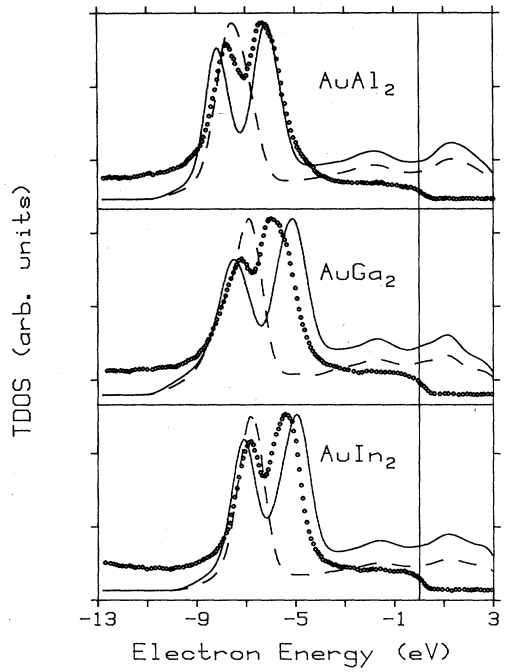

FIG. 7. Comparison between the TDOS for $AuAl_2$, $AuGa_2$, and $AuIn_2$ and the corresponding XPS spectra of Ref. 19, all plotted versus binding energy referenced to the Fermi level. XPS spectra are shown as circles, and only represent occupied states. TDOS corresponding to nonrelativistic and relativistic energy bands are represented as dashed and solid lines, respectively, and represent both occupied and empty states.

ture without increasing the number of fitting parameters. Finally, the *d*-orbital contributions to the wave function of several bands at the Γ and X points of the BZ obtained from the eigenvectors of the parametrized Hamiltonian are listed in Table II, along with those of Bylander *et al.*[15] for $NiSi_2$.

IV. DISCUSSION

As mentioned in Sec. II, the purpose of increasing the number of plane waves in the basis set of the interpolation scheme from the 16 used by Smith[2] to 39 is to recover the flat band ($\Gamma_{2'}-X_3$) in the $AuGa_2$ valence band, and to improve the fit to the higher-energy conduction bands. The rms error obtained after convergence of the original 16 OPW scheme of Smith[2] to 36 energy levels of $AuGa_2$ (Ref. 14) at five symmetry points was 0.54 eV, and the flat band ($\Gamma_{2'}-X_3$) was not well reproduced. When the 39 plane-wave scheme was used to fit the same set of energy eigenvalues, the rms error quickly converged to 0.115 eV within four iterations. However, even with 39 plane waves, the second band with Γ_{15} and the first with Γ_1 symmetry above the Fermi level E_F deviate 1—2 eV from the results of the first-principles calculations for all four compounds. In order to improve the fit to these and other conduction bands, V_{400} and V_{420} pseudopotential terms were included in the Hamiltonian, but they had a negligible effect on the quality of the fits. Improving the fit to these conduction bands may require more plane waves in the basis, more terms in the Hamiltonian (for instance, to explicitly account for the presence of the *d* orbitals of Ga or In in $AuGa_2$ and $AuIn_2$), or both extensions. The above-mentioned Γ_{15} and Γ_1 conduction-band eigenvalues were omitted in the final fitting procedure for all four intermetallics, since including them in the fit increased the rms error greatly, resulted in unreasonably large values of the standard deviation of several of the fitting parameters, and distorted the valence bands.

Another possible improvement would be in the plane-wave—5*d* overlap integrals, which one would not expect to be well approximated by simple spherical Bessel functions. An attempt was made to use single-ζ Slater functions to approximate the radial portion of the 5*d* orbitals, as described in Sec. II. For $NiSi_2$, the rms error in the fit to the APW results using the 39 OPW scheme after three iterations improved slightly when compared to the spherical Bessel function approximation to 0.133 from 0.146 eV

TABLE II. *d*-orbital contribution to the wave function of the bands at Γ and X points (units in %).

	$NiSi_2$			$AuAl_2$		$AuGa_2$		$AuIn_2$	
	Band[a] (eV)	APW[b]	This work	Band (eV)	This work	Band (eV)	This work	Band (eV)	This work
Γ_{12}	−3.56	94	91.0	−7.66	99.1	−6.66	99.8	−6.46	99.9
$\Gamma_{25'}$	−5.24	70	74.4	−7.02	94.9	−7.34	94.1	−6.91	95.8
$\Gamma_{25'}$	1.94	43	25.5	3.02	5.0	3.03	5.8	2.56	4.2
X_5	−3.70	95	98.3	−7.12	99.6	−6.70	99.5	−6.68	99.6
X_3	−7.34	44	45.0	−8.17	87.0	−8.10	79.5	−7.23	87.6
X_3	−0.55	69	54.8	−0.18	12.9	−1.39	20.2	−0.77	12.3
X_1	−7.96	14	13.5	−7.94	91.9	−7.52	95.5	−6.95	99.1
X_1	−3.40	74	66.8	−4.19	6.8	−3.80	1.6	−3.96	0.8
X_1	1.49	32	19.2	1.08	1.3	2.17	0.25	1.11	0.1

[a]Energy referenced with respect to E_F.
[b]From Ref. 15.

without including the Γ_{15} and Γ_1 conduction-band points, but when these points were included, the same difficulty of convergence was encountered. It was found that there were no negative A values using this single-ζ approximation.

In the case of $AuGa_2$, the single-ζ wave functions were not effective in achieving a fit, even if the Γ_{15} and Γ_1 conduction-band points were not included. The rms error for this trial was 0.335 eV after the third iteration, which is about three times larger than that of the Bessel-function approximation. This is perhaps contrary to initial expectations in view of the severe approximation of using the spherical Bessel functions for overlap integrals. In fact, no improvement in the accuracy of the fit occurred when the Slater wave-function approximations were used. This may be because both overlap approximations actually have very similar k dependence for small k, but both may still be poor approximations to describe the exact overlap integrals.

It is useful to compare the energy-band results for the fluorite compounds among each other and with those for the fcc d metals. A common measure of the d-band width, $E(X_1)-E(X_2)$, is 4.8 eV for $NiSi_2$, which is larger than the 4.4-eV bandwidth of paramagnetic fcc Ni even though the larger spacings between Ni atoms in the intermetallic compound might be expected to produce a d-band narrowing. In fact, examination of Table II shows that a significant amount of d-orbital character is present in bands separated by almost 10 eV. Table II also shows that the d-orbital contribution to the various energy bands of $NiSi_2$ calculated using the interpolation scheme agrees very well with the first-principles calculation of Bylander *et al.*[15] Thus the eigenfunctions of the interpolation Hamiltonian are also good approximations to the first-principles results, and perhaps can be used in the calculation of various one-electron properties.

The broadening of the $3d$ bands of $NiSi_2$ with respect to Ni is caused by hybridization effects, since the A parameters of Table I show that the direct d-d interactions are much smaller in the compound than in the metal. The larger lattice constant of the intermetallic compound has the effect of pushing the plane-wave bands downward energetically and increasing the density of plane-wave states below E_F relative to fcc Ni. The d bands are degenerate with some of these additional plane waves, and the mixing that results produces d-like states that are strongly split at Γ and highly dispersive.

A similar comparison of the d-band widths can be made between the Au intermetallic compounds and Au by using the interpolation scheme to generate a nonrelativistic Au band structure. The $5d$-band width $E(X_5)-E(X_3)$ for Au is 4.9 eV, while equivalent band widths for $AuAl_2$, $AuGa_2$, and $AuIn_2$ are 1.05, 1.40, and 0.56 eV, respectively. In this case, the larger lattice constants of the compounds clearly lead to narrower d-band widths in the APW calculations.[14] This is because the $5d$ bands essentially appear in a band-gap region of the plane-wave states, and do not hybridize appreciably with them, as may seem by looking at the d-orbital contributions to the various bands in Table II. Comparing the A parameters of Au and its compounds show that A_1 and A_2, which directly affect the d-band dispersion and thus the width, are very much smaller for the compounds than for Au. The S orthogonalization term and the B hybridization term for the fluorite compounds are also significantly less than those of the fcc metals. However, as observed in the case of $NiSi_2$, this does not necessarily imply that the d bands and plane waves interact weakly. The B values for the Au compounds are generally smaller than those for $NiSi_2$, but the S terms are approximately the same for all four intermetallics. The importance of these terms in the compounds as compared to the fcc elements comes from the higher plane-wave state density in the energy region near the d bands. The values of B_t and B_e for the Au compounds are quite different from one another, unlike the case of elemental Au. This is reflected in the smaller dispersion of e_g bands than that of t_{2g} bands for the Au compounds.

The spin-orbit splitting in the $5d$ transition metals is quite large, but performing a first-principles band-structure calculation including spin orbit and other relativistic effects is a demanding task. However, once a set of parameters for the nonrelativistic interpolation Hamiltonian has been determined, it is relatively straightforward to generate a band structure including spin-orbit coupling using Eq. (6), which only requires one additional parameter. The spin-orbit parameter ξ may either be taken directly from spectroscopic determinations of atomic energy levels, or it may be determined explicitly for the material of interest if ARPES data exist which show the d-band splittings at the Γ point of the BZ.[22] Since ARPES data exist for both $AuGa_2$ and $AuIn_2$,[13] the latter approach was used here.

The ARPES data[13] showed three clearly resolved d bands at Γ, which could be analyzed in terms of the fcc tight-binding Hamiltonian including spin-orbit coupling[12] to yield the values of ξ for $AuGa_2$ and $AuIn_2$ shown in Table I. However, this analysis also showed that the binding energies of the e_g and t_{2g} levels at Γ determined by the APW calculations[14] were incorrect. Therefore, to generate the band structures shown in Figs. 5 and 6, the experimentally determined ξ value was used and the B_0 and Δ parameters of the interpolation Hamiltonian were adjusted to force the band structure to agree with the three experimentally determined d bands at Γ. All the other parameters used in generating the optimized $AuGa_2$ and $AuIn_2$ band structures were the same as those used in Figs. 2 and 3, respectively. The newly determined d bands were less strongly bound and much broader than the APW bands.[14] A rather fascinating observation is that the relative splittings of the $5d$ bands at Γ are very similar for Au, $AuGa_2$, and $AuIn_2$,[13] but the overall d-band width still decreases for this series since the dispersion of the bands decreases with increasing lattice constant. However, for $AuGa_2$ and $AuIn_2$, the d-band width determined experimentally[13] is substantially larger than the APW calculations suggest.

A common method of determining the quality of a band-structure calculation is to compare the energy dependence of the TDOS to spectral features in a valence-band XPS spectrum. Since the TDOS curve for $NiSi_2$ in Fig. 1 agrees in almost every detail with that cal-

culated by Tersoff and Hamann,[23] the procedure for generating the TDOS using the interpolation scheme as described in Sec. II may be used with confidence. In making direct comparisons with XPS data, however, the Gaussian broadening in the TDOS curves should be larger than the 0.3 eV used in Figs. 1—6 in order to account for lifetime and instrumental resolution effects. Using a broadening of 1.0 eV to generate the $NiSi_2$ TDOS produced a curve with one broad feature that agreed very well with reported XPS valence-band spectra.[24,25] Using the same 1.0-eV broadening for the nonrelativistic bands of the Au intermetallic compounds in Figs. 2—4 produced TDOS plots with a single peak in the valence-band region in Fig. 7, which were in severe disagreement with the corresponding XPS spectra of van Attekum *et al.*[19] The experimental XPS d-band features were broader, lower in binding energy, and had a distinct overlapping double-peak shape. However, when the TDOS corresponding to $AuGa_2$ and $AuIn_2$ bands in Figs. 5 and 6, respectively, and the adjusted $AuAl_2$ bands were generated with 1.0-eV broadening as shown in Fig. 7, the agreement with the corresponding XPS spectra was very good. The double peak is apparent in the adjusted TDOS, and the relative heights of the two peaks agree well for all three compounds. The detailed differences between the XPS data and the TDOS curves may be the result of photoelectron cross-section effects.

V. CONCLUSION

The mixed interpolation scheme for fcc d-band metals was extended to include fluorite-structure compounds by using 39 plane waves in the basis set. The band structures for $NiSi_2$, $AuAl_2$, $AuGa_2$, and $AuIn_2$ produced by this scheme were in good agreement with the corresponding first-principles calculations up to 5 eV above the Fermi level, with rms deviations between the first principles and interpolated bands ~ 0.1 eV. The fit to the higher-energy bands was not as good, but can be improved by using more plane waves in the basis set, more terms in the Hamiltonian, or perhaps a better approximation to the plane-wave—d-overlap integrals. Using the interpolation scheme, spin-orbit effects were added in a very direct manner to a nonrelativistic band-structure calculation. Also, it was possible to adjust the parameters of the interpolation Hamiltonian to obtain agreement of the calculated bands at Γ of the BZ with $AuGa_2$ and $AuIn_2$ ARPES data. The TDOS generated using the interpolated bands of $NiSi_2$ and the empirically adjusted bands of $AuAl_2$, $AuGa_2$, and $AuIn_2$ agreed very well with XPS valence-band spectra. In the case of the Au intermetallic compounds, the adjusted d bands were substantially different from those reported by Switendick and Narath,[14] which did not agree with the XPS results.

ACKNOWLEDGMENTS

This project was supported in part by the Office of Naval Research. The computer on which the calculations were performed was purchased in part with funds supplied by National Science Foundation Grant No. CHE79-10965. R.S.W. gratefully acknowledges the Camille and Henry Dreyfus Foundation and the Alfred P. Sloan Foundation for financial support. The authors also thank D. J. Chadi for enlightening discussions.

APPENDIX A: OVERLAP INTEGRALS WITH SLATER ORBITALS

The radial parts of d-wave functions $R_{nd}(r)$ are approximated with single-ζ Slater wave functions,

$$R_{nd}(r)=cr^{n-1}e^{-\zeta r} . \tag{A1}$$

The resulting radial overlap integrals are represented as follows:

$$\int_0^\infty j^2(kr)r^4e^{-\zeta r}dr=\frac{48\zeta k^2}{(\zeta^2+k^2)^4}, \quad n=3 \tag{A2}$$

$$\int_0^\infty j^2(kr)r^5e^{-\zeta r}dr=\frac{48k^2(7\zeta^2-k^2)}{(\zeta^2+k^2)^5}, \quad n=4 \tag{A3}$$

$$\int_0^\infty j^2(kr)r^6e^{-\zeta r}dr=\frac{384k^2(7\zeta^2-3k^2)}{(\zeta^2+k^2)^6}, \quad n=5 . \tag{A4}$$

APPENDIX B: SYMMETRIZING FACTORS

The purpose of the symmetrizing factors is to compensate for the use of a truncated basis set. In this paper the symmetrizing factor F_i corresponding to plane wave k_i has the following form:

$$F_i=\begin{cases}1 & \text{if } k_i^2<560 , \\ 0 & \text{if } k_i^2>700 , \\ 1-(k_i^2-560)^2/19\,600 & \text{otherwise} .\end{cases}$$

The units of k_i are such that the X point in the first BZ is at (0,0,8), as in Smith's scheme.[6] In the region of $560<k_i^2<700$, the symmetrizing factors vary smoothly from 0 to 1.

[1]L. Hodges, H. Ehrenreich, and N. D. Lang, Phys. Rev. **152**, 505 (1966); H. Ehrenreich and L. Hodges, in *Methods in Computational Physics,* edited by B. Adler, S. Fernbach, and M. Roteberg (Academic, New York, 1968), Vol. 8, p. 149.
[2]F. M. Mueller, Phys. Rev. **153**, 659 (1967).
[3]N. V. Smith and L. F. Mattheiss, Phys. Rev. B **9**, 1341 (1974).
[4]N. V. Smith, Phys. Rev. B **19**, 5019 (1979).
[5]R. Lässer, N. V. Smith, and R. L. Benbow, Phys. Rev. B **24**, 1875 (1981).
[6]R. L. Benbow and N. V. Smith, Phys. Rev. B **27**, 3144 (1983).
[7]L. F. Mattheiss, Phys. Rev. B **5**, 290 (1972).
[8]E. Clementi and C. Roetti, At. Data Nucl. Data Tables **14**, 177 (1974).
[9]J. C. Slater and G. F. Koster, Phys. Rev. **94**, 1498 (1954).

[10]G. C. Fletcher and E. P. Wohlfarth, Philos. Mag. **42**, 106 (1951).
[11]G. C. Fletcher, Proc. Phys. Soc. London Sect. A **65**, 192 (1952).
[12]J. Friedel, P. Lenglart, and G. Leman, J. Phys. Chem. Solids **25**, 781 (1964).
[13]J. G. Nelson, W. J. Ginac, S. Kim, J. R. Lince, and R. S. Williams, following paper, Phys. Rev. B **31**, 3469 (1985).
[14]A. C. Switendick and A. Narath, Phys. Rev. Lett. **22**, 1423 (1969).
[15]D. M. Bylander, L. Kleinman, K. Mednick, and W. R. Grise, Phys. Rev. B **26**, 6379 (1982).
[16]Y. J. Chabel, D. R. Hamann, J. E. Rowe, and M. Schlüter, Phys. Rev. B **25**, 7598 (1982).
[17]N. V. Smith, R. Lässer, and S. Chiang, Phys. Rev. B **25**, 793 (1982).
[18]D. J. Chadi and M. L. Cohen, Phys. Rev. B **8**, 5747 (1973).
[19]P. M. Th. M. van Attekum, G. K. Wertheim, G. Grecelius, and J. H. Wernick, Phys. Rev. B **22**, 3998 (1980).
[20]F. Szmulowicz and D. M. Pease, Phys. Rev. B **17**, 3341 (1978).
[21]N. E. Christensen and B. O. Seraphin, Phys. Rev. B **4**, 3321 (1971).
[22]P. S. Wehner, R. S. Williams, S. D. Kevan, D. Denley, and D. A. Shirley, Phys. Rev. B **19**, 6164 (1979).
[23]J. Tersoff and D. R. Hamann, Phys. Rev. B **28**, 1168 (1983).
[24]A. Franciosi and J. H. Weaver, Phys. Rev. B **26**, 546 (1982).
[25]T. T. A. Nguyen and R. Cinti, Phys. Scr. T **4**, 176 (1983).